

SUPPLEMENTARY MATERIAL

for

Phenotypic integration and modularity drives skull shape divergence in the Arctic fox (*Vulpes lagopus*) from the Commander islands

Alberto Martín-Serra, Olga Nanova, Ceferino Varón-González, Germán Ortega, Borja

Figueirido

Supplementary Results

Although there is not strong sexual size dimorphism in the Arctic fox (29), we performed a Procrustes ANOVA to explore if differences in the number of males/females among populations affected the strength of integration and modularity. The Procrustes ANOVA revealed that differences in the number of males and females among populations does not bias patterns of integration and modularity (Table S5).

Supplementary Figures and Tables

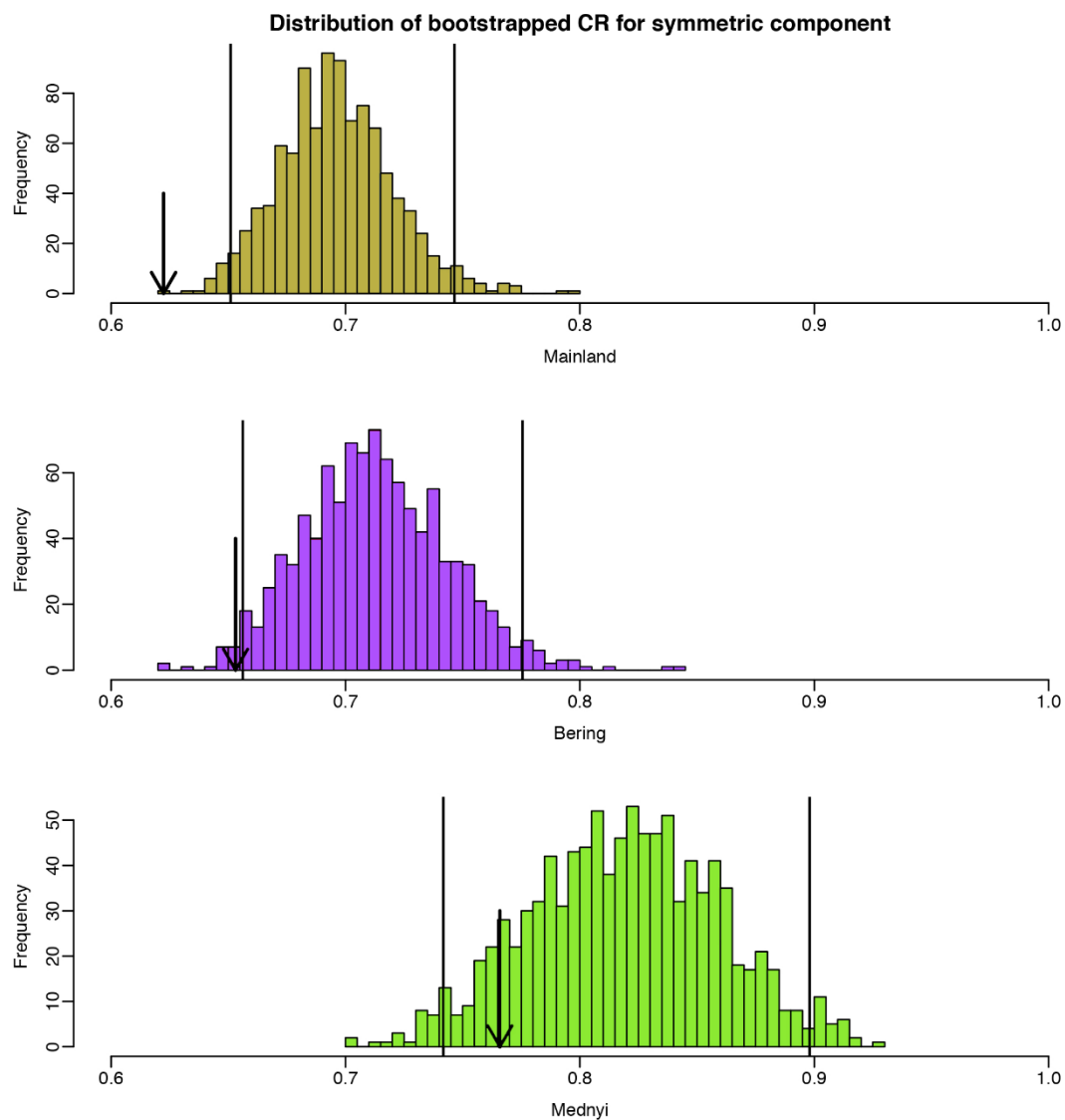


Figure S1. Histograms obtained from the bootstrap analyses on CR values for the symmetric component of shape. Each graph shows the distribution of CR values (1000 iterations) for each population. Black arrows indicate the observed CR values and the vertical lines indicate the 95% of confidence intervals.

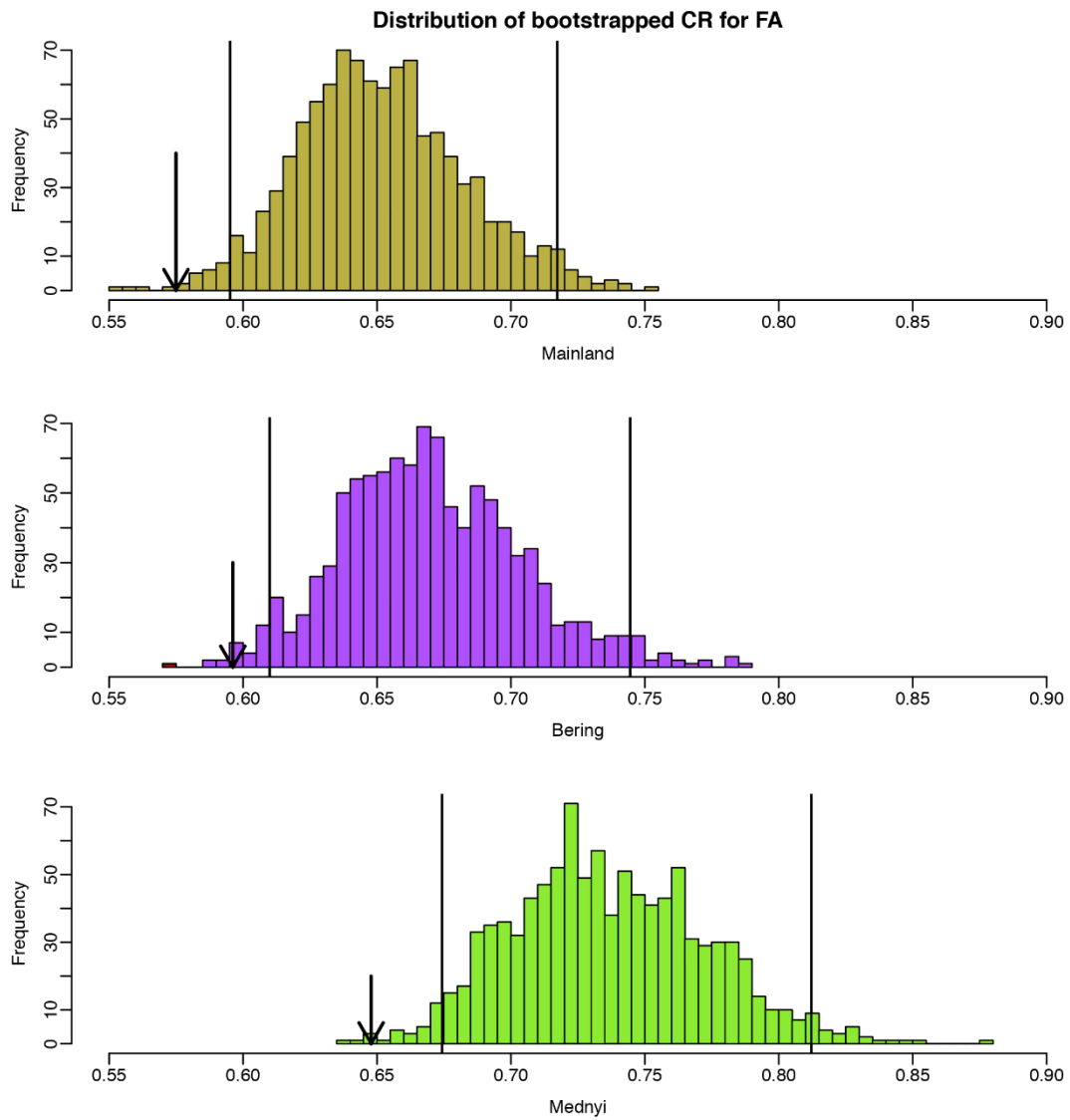


Figure S2. Histograms obtained from the bootstrap analyses on CR values for FA. Each graph shows the distribution of CR values (1000 iterations) for each population. Black arrows indicate the observed CR values and the vertical lines indicate the 95% of confidence intervals.

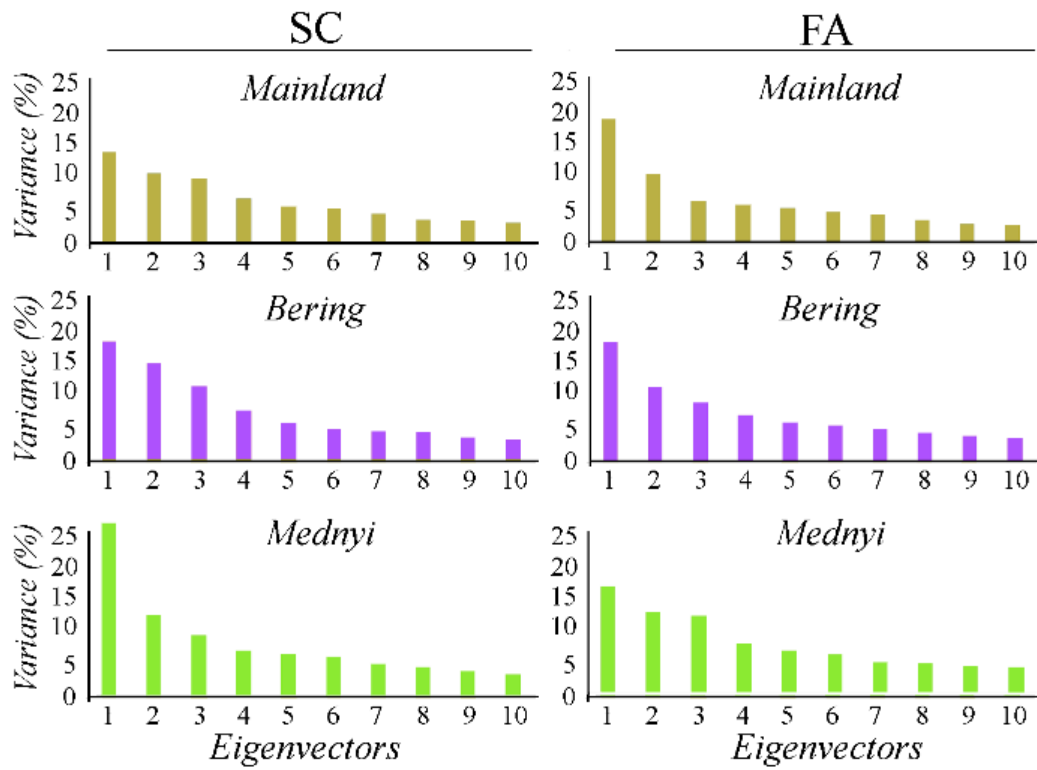


Figure S3. Histograms showing the percentage of variance explained for by each eigenvector obtained from the PCAs of the symmetric component (SC) and of fluctuating assymetry (FA) of shape. See also Table S9.

Table S1. Museum numbers, sex and population of the skulls analysed in this article.

| Museum number | Sex | Population |
|----------------------|------------|-------------------|
| S-5923 | Female | Bering |
| S-11963 | Female | Bering |
| S-11965 | Female | Bering |
| S-11970 | Female | Bering |
| S-11974 | Female | Bering |
| S-11991 | Male | Bering |
| S-12059 | Female | Bering |
| S-12060 | Female | Bering |
| S-30339 | Female | Bering |
| S-30355 | Female | Bering |
| S-30356 | Female | Bering |
| S-30361 | Male | Bering |
| S-30367 | Male | Bering |
| S-30371 | Female | Bering |
| S-30378 | Male | Bering |
| S-42779 | Female | Bering |
| S-166344 | Male | Bering |
| S-166345 | Female | Bering |
| S-166362 | Male | Bering |
| S-166406 | Male | Bering |
| S-166427 | Female | Bering |
| S-166449 | Male | Bering |
| S-166464 | Male | Bering |
| S-166496 | Female | Bering |

| | | |
|-----------------|--------|--------|
| S-166528 | Female | Bering |
| S-166531 | Female | Bering |
| S-166539 | Male | Bering |
| S-166551 | Male | Bering |
| S-166556 | Male | Bering |
| S-166595 | Female | Bering |
| S-166609 | Male | Bering |
| S-166611 | Male | Bering |
| S-166618 | Male | Bering |
| S-166621 | Male | Bering |
| S-166623 | Male | Bering |
| S-166634 | Male | Bering |
| S-166636 | Male | Bering |
| S-166642 | Male | Bering |
| S-166645 | Male | Bering |
| S-166646 | Female | Bering |
| S-166648 | Female | Bering |
| S-166652 | Female | Bering |
| S-166654 | Male | Bering |
| S-166659 | Female | Bering |
| S-166664 | Male | Bering |
| S-166665 | Female | Bering |
| S-166668 | Female | Bering |
| S-166669 | Female | Bering |
| S-166670 | Male | Bering |
| S-167009 | Male | Bering |
| S-167017 | Male | Bering |

| | | |
|----------------|--------|--------|
| S-5928 | Female | Mednyi |
| S-5929 | Female | Mednyi |
| S-5930 | Female | Mednyi |
| S-5931 | Female | Mednyi |
| S-5932 | Male | Mednyi |
| S-5934 | Male | Mednyi |
| S-6166 | Male | Mednyi |
| S-6168 | Female | Mednyi |
| S-6169 | Male | Mednyi |
| S-6170 | Female | Mednyi |
| S-12007 | Male | Mednyi |
| S-12010 | Male | Mednyi |
| S-12015 | Male | Mednyi |
| S-12025 | Male | Mednyi |
| S-12026 | Male | Mednyi |
| S-12027 | Male | Mednyi |
| S-12030 | Male | Mednyi |
| S-12031 | Male | Mednyi |
| S-12033 | Male | Mednyi |
| S-12034 | Male | Mednyi |
| S-12037 | Female | Mednyi |
| S-12038 | Female | Mednyi |
| S-12041 | Male | Mednyi |
| S-12043 | Male | Mednyi |
| S-12045 | Male | Mednyi |
| S-12046 | Female | Mednyi |
| S-12049 | Female | Mednyi |

| | | |
|-----------------|--------|----------|
| S-12050 | Male | Mednyi |
| S-12051 | Female | Mednyi |
| S-12053 | Male | Mednyi |
| S-12056 | Male | Mednyi |
| S-69547 | Female | Mednyi |
| S-167038 | Female | Mednyi |
| S-170790 | Female | Mednyi |
| S-179789 | Female | Mednyi |
| S-179792 | Female | Mednyi |
| S-179793 | Male | Mednyi |
| S-188218 | Male | Mednyi |
| S-191289 | Male | Mednyi |
| S-191488 | Female | Mednyi |
| S-97487 | Male | Mainland |
| S-97518 | Male | Mainland |
| S-97523 | Male | Mainland |
| S-97524 | Male | Mainland |
| S-97526 | Male | Mainland |
| S-97531 | Male | Mainland |
| S-97533 | Male | Mainland |
| S-97534 | Male | Mainland |
| S-97545 | Male | Mainland |
| S-97546 | Male | Mainland |
| S-97547 | Male | Mainland |
| S-97548 | Male | Mainland |
| S-97553 | Male | Mainland |
| S-97559 | Male | Mainland |

| | | |
|----------------|--------|----------|
| S-97564 | Female | Mainland |
| S-97567 | Female | Mainland |
| S-97572 | Female | Mainland |
| S-97577 | Female | Mainland |
| S-97578 | Female | Mainland |
| S-97581 | Female | Mainland |
| S-97584 | Female | Mainland |
| S-97586 | Female | Mainland |
| S-97603 | Female | Mainland |
| S-97606 | Female | Mainland |
| S-97614 | Male | Mainland |
| S-97617 | Female | Mainland |
| S-97624 | Male | Mainland |
| S-97629 | Female | Mainland |
| S-97630 | Female | Mainland |
| S-97638 | Female | Mainland |
| S-97641 | Female | Mainland |
| S-97643 | Male | Mainland |
| S-97650 | Female | Mainland |
| S-97667 | Male | Mainland |
| S-97669 | Male | Mainland |
| S-97671 | Male | Mainland |
| S-97689 | Female | Mainland |
| S-97693 | Male | Mainland |
| S-97694 | Male | Mainland |
| S-97695 | Female | Mainland |
| S-97734 | Female | Mainland |

| | | |
|----------------|--------|----------|
| S-97739 | Male | Mainland |
| S-97741 | Female | Mainland |
| S-97743 | Female | Mainland |
| S-97744 | Male | Mainland |
| S-97746 | Female | Mainland |
| S-97747 | Male | Mainland |
| S-97748 | Male | Mainland |
| S-97751 | Female | Mainland |
| S-97760 | Female | Mainland |

Table S2. Anatomical criteria used in this article to digitize de 52 LMs on the Artic fox skulls. See also Figure S1.

| <i>L</i> | <i>Definition</i> |
|----------|--|
| <i>m</i> | |
| 0 | Occiput |
| 1 | Junction of parietal and frontal sutures at the sagittal crest. |
| 2 | Tip of the right postorbital process. |
| 3 | Tip of the left postorbital process. |
| 4 | Most ventral point of the right lacrimal foramen. |
| 5 | Most ventral point of the left lacrimal foramen. |
| 6 | Most anterior point of the junction of both nasal bones suture. |
| 7 | Prostion. |
| 8 | Tip of the right preorbital process. |
| 9 | Tip of the left preorbital process. |
| 10 | Posteroventral point of the righth jugal and squamosal bones. |
| 11 | Posteroventral point of the left jugal and squamosal bones. |
| 12 | Posteroventral point of both palatine bones. |
| 13 | Posteroventral point of the left third molar. |
| 14 | Interdental gap between the second and third left molars |
| 15 | Interdental gap between the first and second left molars |
| 16 | Interdental gap between the left third premolar and first molar |
| 17 | Interdental gap between the left second premolar and third premolar |
| 18 | Interdental gap between the left first premolar and second premolar |
| 19 | Interdental gap between the left first premolar and the canine |
| 20 | Most antero-dorsal point of the left canine |
| 21 | Most postero-dorsal point of the left third incisive |
| 22 | Most postero-dorsal point of the right third incisive |
| 23 | Most antero-dorsal point of the right canine |
| 24 | Interdental gap between the right first premolar and the canine |
| 25 | Interdental gap between the right first premolar and second premolar |
| 26 | Interdental gap between the right second premolar and third premolar |
| 27 | Interdental gap between the right third premolar and first molar |
| 28 | Interdental gap between the first and second right molars |
| 29 | Interdental gap between the second and third right molars |
| 30 | Posteroventral point of the right third molar. |

- 31 Posterior margin of the right incisive foramen at the premaxilar bone.
 - 32 Posterior margin of the left incisive foramen at the premaxilar bone.
 - 33 Anterior margin of the right lacerum foramen of the tympanic bulla.
 - 34 Anterior margin of the left lacerum foramen of the tympanic bulla.
 - 35 Ventral junction of the right paracondylar process and the tympanic bulla.
 - 36 Ventral junction of the left paracondylar process and the tympanic bulla.
 - 37 Ventral junction of the right and left occipital condyles.
 - 38 Dorsal margin of the left infraorbital foramen.
 - 39 Dorsal margin of the right infraorbital foramen.
 - 40 Ventral tip of the left postglenoid process.
 - 41 Ventral tip of the right postglenoid process.
 - 42 Most lateral point of the left glenoid fossa.
 - 43 Most lateral point of the right glenoid fossa.
 - 44 Ventral margin of the left auditory meatus.
 - 45 Dorsal point of the left auditory meatus.
 - 46 Ventral margin of the right auditory meatus.
 - 47 Dorsal point of the right auditory meatus.
 - 48 Most medial point of the left glenoid fossa.
 - 49 Most medial point of the right glenoid fossa.
 - 50 Ventral margin of the left optic foramen.
 - 51 Ventral margin of the right optic foramen.
-

Table S3. Skull shape asymmetry for each population of Arctic foxes. The analysis of variance was performed from the residuals of shape on size obtained for each population. Abbreviations: *ind.* individuals; *side.* effect of directional asymmetry; *ind:side.* effect of fluctuating asymmetry; *ind:side:replicate.* effects of differences between replicates (error). We used a separate permutation test to determine statistical significance of each effect.

| | <i>Df</i> | <i>SS</i> | <i>MS</i> | <i>Rsq</i> | <i>F</i> | <i>Z</i> | <i>Pr(>F)</i> |
|---------------------------|-----------|-----------|-----------|------------|----------|----------|------------------|
| Mainland | | | | | | | |
| <i>ind</i> | 50 | 52.791 | 1.0558 | 0.49649 | 2.2058 | -4.0091 | 0.001 |
| <i>side</i> | 1 | 12.763 | 12.7634 | 0.12004 | 26.6658 | 8.8106 | 0.001 |
| <i>ind:side</i> | 50 | 23.932 | 0.4786 | 0.22508 | 2.899 | 28.4328 | 0.001 |
| <i>ind:side:replicate</i> | 102 | 16.841 | 0.1651 | 0.15839 | | | |
| <i>Total</i> | 203 | 106.327 | | | | | |
| Bering | | | | | | | |
| <i>ind</i> | 50 | 47.209 | 0.9442 | 0.44192 | 2.2512 | -0.5915 | 0.001 |
| <i>side</i> | 1 | 13.312 | 13.3123 | 0.12462 | 31.7411 | 9.6361 | 0.001 |
| <i>ind:side</i> | 50 | 20.97 | 0.4194 | 0.1963 | 1.6885 | 25.5619 | 0.001 |
| <i>ind:side:replicate</i> | 102 | 25.335 | 0.2484 | 0.23716 | | | |
| <i>Total</i> | 203 | 106.827 | | | | | |
| Mednyi | | | | | | | |
| <i>ind</i> | 31 | 26.825 | 0.8653 | 0.37339 | 1.5389 | -6.4092 | 0.001 |
| <i>side</i> | 1 | 13.558 | 13.558 | 0.18872 | 24.1123 | 7.1988 | 0.001 |
| <i>ind:side</i> | 31 | 17.431 | 0.5623 | 0.24263 | 2.5654 | 25.1085 | 0.001 |
| <i>ind:side:replicate</i> | 64 | 14.027 | 0.2192 | 0.19525 | | | |
| <i>Total</i> | 127 | 71.841 | | | | | |

Table S4. Results of the integration test for the symmetric component of shape (SC) and for fluctuating asymmetry (FA) obtained from 2B-PLS for each population of Arctic foxes. P-values of the two-sample Z-tests using the pooled standard error from the sampling distributions of the PLS analyses. For the effect sizes (Z-scores) of each population see text.

| | SC | | | FA | | |
|-----------------|-----------------|---------------|---------------|-----------------|---------------|---------------|
| | <i>Mainland</i> | <i>Bering</i> | <i>Mednyi</i> | <i>Mainland</i> | <i>Bering</i> | <i>Mednyi</i> |
| <i>Mainland</i> | - | 0.00 | 0.00 | - | 0.000 | 0.000 |
| <i>Bering</i> | 0.00 | - | 0.33 | 0.000 | - | 0.325 |
| <i>Mednyi</i> | 0.00 | 0.33 | - | 0.000 | 0.325 | - |

Table S5. Analyses of variance for sexes for the symmetric component of shape (SC) and fluctuating asymmetry (FA). Abbreviation: *Sex*. effect of differences between sexes; *Pop*. effect of different populations; *Sex:Pop*. interaction between sexes and populations.

| SC | | | | | | | |
|------------------|-----|----------|----------|---------|---------|---------|--------|
| | Df | SS | MS | Rsq | F | Z | Pr(>F) |
| <i>Sex</i> | 1 | 0.001778 | 0.001778 | 0.01531 | 2.99 | 2.8738 | 0.005 |
| <i>Pop</i> | 2 | 0.036402 | 0.018201 | 0.31333 | 30.6059 | 11.6281 | 0.001 |
| <i>Sex:Pop</i> | 2 | 0.001879 | 0.00094 | 0.01617 | 1.5799 | 4.0659 | 0.001 |
| <i>Residuals</i> | 128 | 0.07612 | 0.000595 | 0.6552 | | | |
| <i>Total</i> | 133 | 0.116179 | | | | | |
| FA | | | | | | | |
| | Df | SS | MS | Rsq | F | Z | Pr(>F) |
| <i>Sex</i> | 1 | 0.000353 | 0.000353 | 0.00697 | 0.9498 | -0.071 | 0.505 |
| <i>Pop</i> | 2 | 0.001748 | 0.000874 | 0.03457 | 2.3543 | 4.5033 | 0.001 |
| <i>Sex:Pop</i> | 2 | 0.00095 | 0.000475 | 0.01879 | 1.2799 | 1.5775 | 0.055 |
| <i>Residuals</i> | 128 | 0.04751 | 0.000371 | 0.93967 | | | |
| <i>Total</i> | 133 | 0.05056 | | | | | |

Table S6. Results of disparity analysis (Procrustes variance) for each population of Arctic foxes. P-values of the pairwise comparisons of disparity values among populations for both the symmetric component of shape (SC) and for fluctuating asymmetry (FA). For disparity values of each population see text.

| | SC | | | FA | | |
|-----------------|-----------------|---------------|---------------|-----------------|---------------|---------------|
| | <i>Mainland</i> | <i>Bering</i> | <i>Mednyi</i> | <i>Mainland</i> | <i>Bering</i> | <i>Mednyi</i> |
| <i>Mainland</i> | - | 0.285 | 0.014 | - | 0.419 | 0.001 |
| <i>Bering</i> | 0.285 | - | 0.001 | 0.419 | - | 0.001 |
| <i>Mednyi</i> | 0.014 | 0.001 | - | 0.001 | 0.001 | - |

Table S7. Angles between the first three eigenvectors obtained from a PCA per population for SC and FA. The p-values for the pairwise comparisons between eigenvectors are given within parentheses. Non-significant p-values indicate that both eigenvectors are orthogonal, and therefore, the shape variation accounted for by them is different.

| SC | Bering PC1 | Bering PC2 | Bering PC3 |
|---------------------|-------------------|-------------------|-------------------|
| Mainland PC1 | 67.537 (0.00056) | 52.302 (<0.00001) | 76.853 (0.04522) |
| Mainland PC2 | 65.400 (0.00015) | 79.143 (0.09865) | 57.461 (<0.00001) |
| Mainland PC3 | 50.023 (<0.00001) | 70.181 (0.00239) | 68.667 (0.00106) |
| | MednyiPC1 | MednyiPC2 | MednyiPC3 |
| Mainland PC1 | 48.600 (<0.00001) | 75.697 (0.02922) | 88.900 (0.86753) |
| Mainland PC2 | 81.487 (0.19588) | 59.248 (<0.00001) | 74.472 (0.01781) |
| Mainland PC3 | 66.266 (0.00026) | 87.809 (0.73971) | 79.470 (0.10927) |
| | MednyiPC1 | MednyiPC2 | MednyiPC3 |
| Bering PC1 | 87.549 (0.71002) | 51.909 (<0.00001) | 66.604 (0.00032) |
| Bering PC2 | 67.675 (0.00060) | 81.269 (0.18461) | 76.993 (0.04757) |
| Bering PC3 | 83.877 (0.35262) | 65.981 (0.00022) | 69.411 (0.00159) |
| FA | Bering PC1 | Bering PC2 | Bering PC3 |
| Mainland PC1 | 42.278 (<0.00001) | 72.138 (0.00831) | 83.686 (0.35430) |
| Mainland PC2 | 65.848 (0.00033) | 61.855 (0.00003) | 88.080 (0.77843) |
| Mainland PC3 | 80.535 (0.16447) | 87.093 (0.67001) | 89.250 (0.91249) |
| | MednyiPC1 | MednyiPC2 | MednyiPC3 |
| Mainland PC1 | 46.019 (<0.00001) | 85.088 (0.47131) | 87.919 (0.76039) |
| Mainland PC2 | 82.197 (0.29868) | 79.902 (0.13788) | 72.435 (0.00947) |
| Mainland PC3 | 88.013 (0.77088) | 83.868 (0.36839) | 88.250 (0.79757) |
| | MednyiPC1 | MednyiPC2 | MednyiPC3 |
| Bering PC1 | 48.114 (<0.00001) | 72.078 (0.00809) | 77.781 (0.07226) |
| Bering PC2 | 79.428 (0.12026) | 80.373 (0.15730) | 72.813 (0.01115) |
| Bering PC3 | 83.332 (0.32797) | 89.114 (0.89667) | 69.740 (0.00269) |

Table S8. Percentages of variance explained for by each eigenvector obtained from the PCAs performed for each population separately from SC and FA. See also Figure 3.

| PC | SC Mainland | SC Bering | SC Mednyi | FA Mainland | FA Bering | FA Mednyi |
|----|-------------|-----------|-----------|-------------|-----------|-----------|
| 1 | 13.74000 | 16.99000 | 25.08000 | 19.07900 | 17.06700 | 16.14000 |
| 2 | 10.49100 | 13.83700 | 11.74000 | 10.88800 | 10.65300 | 12.15700 |
| 3 | 9.82500 | 10.48300 | 8.70100 | 6.84700 | 8.36400 | 11.61000 |
| 4 | 6.73600 | 7.09400 | 6.51300 | 6.24100 | 6.60800 | 7.31600 |
| 5 | 5.59800 | 5.30900 | 5.97500 | 5.68600 | 5.63500 | 6.26700 |
| 6 | 5.26900 | 4.39500 | 5.53700 | 5.09300 | 5.10800 | 5.76800 |
| 7 | 4.58100 | 4.09200 | 4.50100 | 4.76000 | 4.62200 | 4.52400 |
| 8 | 3.63500 | 4.00900 | 4.10800 | 3.94800 | 4.14600 | 4.36200 |
| 9 | 3.45600 | 3.25700 | 3.42500 | 3.40800 | 3.57700 | 4.00000 |
| 10 | 3.15500 | 2.93500 | 3.04400 | 3.19900 | 3.27500 | 3.72500 |
| 11 | 2.95600 | 2.73300 | 2.55300 | 2.86400 | 2.94900 | 3.34000 |
| 12 | 2.62400 | 2.43400 | 2.20900 | 2.63200 | 2.57900 | 2.57000 |
| 13 | 2.39300 | 2.12700 | 1.95400 | 2.30000 | 2.37900 | 2.21100 |
| 14 | 2.34900 | 1.91900 | 1.83500 | 2.26000 | 2.24100 | 2.14900 |
| 15 | 2.16800 | 1.77900 | 1.56300 | 1.98000 | 1.99200 | 1.95300 |
| 16 | 1.92100 | 1.59800 | 1.43000 | 1.81800 | 1.92600 | 1.71300 |
| 17 | 1.82100 | 1.36300 | 1.31500 | 1.71700 | 1.56000 | 1.46900 |
| 18 | 1.58100 | 1.24500 | 1.28000 | 1.61900 | 1.45800 | 1.29100 |
| 19 | 1.49400 | 1.09300 | 1.11400 | 1.44600 | 1.37800 | 1.24600 |
| 20 | 1.42500 | 0.99100 | 1.00100 | 1.40000 | 1.34200 | 1.01800 |
| 21 | 1.31200 | 0.87700 | 0.89500 | 1.22800 | 1.27800 | 0.86600 |
| 22 | 1.12400 | 0.84800 | 0.76700 | 1.16100 | 1.13700 | 0.78300 |
| 23 | 1.08800 | 0.78100 | 0.74300 | 1.03600 | 0.95800 | 0.67200 |
| 24 | 1.00500 | 0.73900 | 0.58400 | 0.85900 | 0.88300 | 0.62000 |
| 25 | 0.87600 | 0.68900 | 0.51000 | 0.73500 | 0.83800 | 0.50800 |
| 26 | 0.76500 | 0.64000 | 0.41700 | 0.71600 | 0.70400 | 0.48900 |
| 27 | 0.70500 | 0.60800 | 0.34700 | 0.66200 | 0.67800 | 0.38500 |
| 28 | 0.62700 | 0.54700 | 0.32800 | 0.59600 | 0.62900 | 0.29500 |
| 29 | 0.55200 | 0.52300 | 0.31600 | 0.54800 | 0.57500 | 0.22500 |
| 30 | 0.53800 | 0.49700 | 0.21600 | 0.47100 | 0.56500 | 0.18000 |
| 31 | 0.48400 | 0.41200 | 0.00000 | 0.45000 | 0.48100 | 0.14700 |
| 32 | 0.44300 | 0.37100 | 0.00000 | 0.43700 | 0.43700 | 0.00000 |
| 33 | 0.40300 | 0.34300 | 0.00000 | 0.34200 | 0.36800 | 0.00000 |
| 34 | 0.36900 | 0.30300 | 0.00000 | 0.28800 | 0.32200 | 0.00000 |
| 35 | 0.31400 | 0.29700 | 0.00000 | 0.24900 | 0.29700 | 0.00000 |
| 36 | 0.31000 | 0.25100 | 0.00000 | 0.21700 | 0.25800 | 0.00000 |
| 37 | 0.28700 | 0.23900 | 0.00000 | 0.19800 | 0.21500 | 0.00000 |
| 38 | 0.25200 | 0.20400 | 0.00000 | 0.18100 | 0.14500 | 0.00000 |
| 39 | 0.22100 | 0.19700 | 0.00000 | 0.12700 | 0.12000 | 0.00000 |
| 40 | 0.21100 | 0.16900 | 0.00000 | 0.11300 | 0.11500 | 0.00000 |
| 41 | 0.17700 | 0.14800 | 0.00000 | 0.09700 | 0.07000 | 0.00000 |

| | | | | | | |
|----|---------|---------|---------|---------|---------|---------|
| 42 | 0.15000 | 0.12500 | 0.00000 | 0.05500 | 0.04900 | 0.00000 |
| 43 | 0.12700 | 0.11000 | 0.00000 | 0.02700 | 0.01400 | 0.00000 |
| 44 | 0.10500 | 0.10000 | 0.00000 | 0.01500 | 0.00200 | 0.00000 |
| 45 | 0.10100 | 0.08800 | 0.00000 | 0.01000 | 0.00000 | 0.00000 |
| 46 | 0.09000 | 0.07500 | 0.00000 | 0.00000 | 0.00000 | 0.00000 |
| 47 | 0.06700 | 0.06100 | 0.00000 | 0.00000 | 0.00000 | 0.00000 |
| 48 | 0.04300 | 0.04800 | 0.00000 | 0.00000 | 0.00000 | 0.00000 |
| 49 | 0.03500 | 0.02300 | 0.00000 | 0.00000 | 0.00000 | 0.00000 |